Macrophage MST1/2 Disruption Impairs Post-Infarction Cardiac Repair via LTB4

Mingming Liu[1,7,#], Meng Yan[1,6,#], Jinlong He[2,#], Huizhen Lv[1,2,#], Zhipeng Chen[2], Liyuan Peng[5], Wenbin Cai[2], Fang Yao[4], Chen Chen[5], Lei Shi[3], Kai Zhang[3], Xu Zhang[2], Dao-Wen Wang[5], Li Wang[4], Yi Zhu[2], Ding Ai[1,2]

[1]Tianjin Key Laboratory of Ion and Molecular Function of Cardiovascular Diseases, Tianjin Institute of Cardiology, State Key Laboratory of Experimental Hematology, National Clinical Research Center for Blood Diseases, Key Laboratory of Immune Microenvironment and Disease (Ministry of Education), Tianjin Medical University, Tianjin; [2]Physiology and Pathophysiology, Tianjin Medical University, Tianjin; [3]Biochemistry and Molecular Biology, School of Basic Medical Sciences, Tianjin Medical University, Tianjin; [4]State Key Laboratory of Cardiovascular Disease, Fuwai Hospital, National Center for Cardiovascular Diseases, Chinese Academy of Medical Sciences and Peking Union Medical College; [5]Cardiology, Department of Internal Medicine, Tongji Hospital, Tongji Medical College, Huazhong University of Science & Technology, Wuhan; [6]The First Affiliated Hospital of Soochow University Department of Pathology, Soochow University, Suzhou; [7]Neurology, Tianjin Neurological Institute, Tianjin Medical University General Hospital, Tianjin.

[#]These authors contributed equally to this study.

***Running title*:** Macrophage MST1 Regulates Cardiac Repair

Subject Terms:
Animal Models of Human Disease
Basic Science Research
Cell Signaling/ Signal Transduction
Inflammation
Vascular Biology

Author correspondence to:
Dr. Ding Ai
Department of Physiology and Pathophysiology
Tianjin Medical University
22 Qixiangtai Road
Tianjin, China, 300070.
edin2000cn@163.com

ABSTRACT

Rationale: Timely inhibition of inflammation and initiation of resolution are important to repair injured tissues. Mammalian STE20-like protein kinase 1/2 (MST1/2) acts as a regulator of macrophage-associated immune responses to bacterial infections. However, the role of MST1/2 in regulating macrophage phenotype and function in myocardial infarction (MI) remains unclear.

Objective: To determine the function and underlying mechanism of macrophage MST1/2 in cardiac repair post-MI.

Methods and Results: Using *LysMCre*-mediated *Mst1/2*-deficient mice, we found that MST1 deficiency exacerbated cardiac dysfunction after MI. Single-cell RNA sequencing assay indicated that the effect was attributed to a shift of macrophage subtypes from those expressing *Cxcl2* and *Cd163* toward *Ccl2* and *Ccl4* expression. Mass spectrometry identified leukotriene B4 (LTB4) as the lipid mediator that was upregulated in the absence of MST1. We found that MST1 phosphorylated 5-lipoxygenase (5-LOX) at its T218 residue, disrupting the interaction between 5-LOX and 5-LOX-activating protein, resulting in a reduction of LTB4 production. In contrast, a 5-LOX^{T218A} variant showed no response to MST1. Moreover, treatment of peritoneal macrophages with LTB4 or medium conditioned by *Mst1*-deficient macrophages resulted in high *Ccl2* and *Ccl4* expression and low *Cxcl2* and *Cd163* expression, except when the cells were co-treated with the LTB4 receptor 1 (BLT1) antagonist CP105696. Furthermore, CP105696 ameliorated cardiac dysfunction in *LysMCre*-mediated *Mst1/2*-deficient mice and enhanced cardiac repair in wild-type mice treated with XMU-MP-1 after MI.

Conclusions: Taken together, our results demonstrate that inhibition of MST1/2 impaired post-MI repair through activating macrophage 5-LOX–LTB4–BLT1 axis.

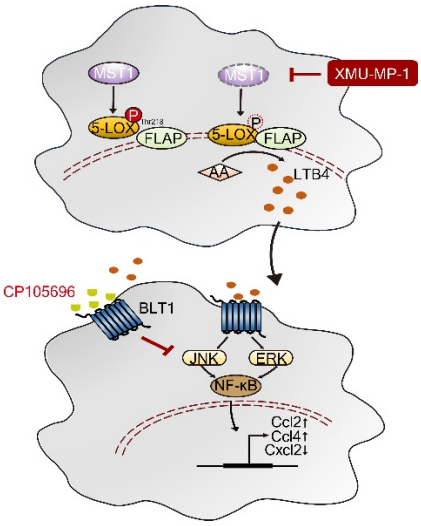

Nonstandard Abbreviations and Acronyms:

5-LOX	5-lipoxygenase
BLT1	Leukotriene B4 receptor 1
Ccl2	C-C motif chemokine ligand 2
Ccl4	C-C motif chemokine ligand 4
CM	Conditioned medium
CO	Cardiac output
Cxcl2	C-X-C motif chemokine ligand 2
EF	Ejection fraction
FLAP	5-lipoxygenase-activating protein
FS	Fractional shortening
LC-MS/MS	Liquid chromatography-tandem mass spectrometry
LTB4	Leukotriene B4
LVEDV	Left ventricular end-diastolic volume
LVESV	Left ventricular end-systolic volume
MI	Myocardial infarction
MST1	Mammalian STE20-like protein kinase 1
STEMI	ST-elevation myocardial infarction
YAP	Yes-associated protein

INTRODUCTION

Acute myocardial infarction (MI) is one of the most frequent causes of myocardial injury. Although early revascularization therapy and drug treatment promote cardiac repair after ischemia and improve the survival rate of individuals with MI; however, some patients experience heart failure. The repair of injured tissues depends on the timely suppression of inflammation. Cardiac acute inflammation is characterized by the sequential release of inflammatory mediators, resulting in the immediate influx of polymorphonuclear leukocytes, followed by phagocytosis, monocytes and macrophages, along with proteolysis, angiogenesis, and collagen deposition [1, 2]. However, overactive, prolonged, or spatially expanded inflammatory reactions lead to serious damage and dysfunction. The balance of fatty-acid-derived proinflammatory mediators and specialized mediators of resolution during acute inflammation regulates the duration of the inflammatory response and the timing of tissue resolution [3, 4].

Ischemia has a stimulatory effect on the expression and activity of enzymes that catalyze lipid oxidation of the *n*-6 fatty acid precursor arachidonic acid [5]. As an important source of these lipid mediators, macrophages undergo metabolic reprogramming toward the LOX pathway during atherogenesis [6]. As an important source of these lipid mediators, macrophages undergo metabolic reprogramming toward the LOX pathway during atherogenesis [7-9]. The functions of leukotrienes in metabolic fate and regenerative potential in the heart after MI are elusive.

The Hippo pathway is important to control cell proliferation and differentiation [10-12], and is involved in tissue regeneration and oncogenesis in the liver, intestine, and heart [13]. The serine/threonine kinases mammalian STE20-like kinase 1 (MST1) and MST2 are essential components of the Hippo pathway. However, the phenotypes of mice with conditional knockouts of the genes encoding these proteins are dependent on physiological context [14]. Full-length MST1 localized predominantly in the cytoplasm because of carboxy-terminal nuclear export signals. However, after treatment with leptomycin B, nuclear accumulation is observed as an inhibitor of the nuclear export signals receptor [15]. Cardiac MST1 is activated by pathological stimuli, such as hypoxia/reoxygenation in vitro and ischemia/reperfusion in vivo [16]. Cardiac-specific inhibition of endogenous MST1 prevents apoptosis of cardiomyocytes and cardiac dysfunction after MI [17], which might enhance the Hippo pathway downstream effector Yes-associated protein (YAP) activity [18-21]. Thus, a pharmacological inhibitor of MST1/2 (XMU-MP-1) has therapeutic potential for promoting cardiac repair following MI. Loss-of-function mutation of the gene encoding MST1 (*STK4*, also known as *MST1*) is associated with immunodeficiency and causes symptoms, such as recurrent bacterial and viral infections and lymphopenia in humans [22, 23]. Pharmacological inhibition of mammalian STE20-like protein kinase 1/2 (MST1/2) with XMU-MP-1 might augment tissue regeneration by suppressing apoptosis and increasing cell proliferation. However, MST1 has anti-inflammatory activity in immune cells, its inhibition may result in therapy failure. Here, we identified an approach with the potential of protecting against cardiac inflammation resulting from the inhibition of MST1 in macrophages. Although monocytes and macrophages contribute to cardiac injury, YAP is expressed at a low level in these cells [24], so the downstream roles of MST1/2 in macrophages might differ from those in cardiomyocytes. Therefore, it is vital to dissect the function and underlying mechanism of macrophage MST1/2 in regulating dynamic transition between inflammation and repair in the heart following MI.

In this study, we found that pharmacological and genetic inhibition of MST1/2 resulted in the reprogramming of macrophages metabolism of arachidonic-acid-derived lipid mediators to exacerbate cardiac dysfunction post-MI. Our data demonstrated that MST1 phosphorylated 5-LOX at the T218 residue, which prevented its interaction with 5-LOX-activating protein (FLAP) in the nuclear membrane, and reduced leukotriene B4 (LTB4) production. To prevent the proinflammatory effect of LTB4 induction resulting from inhibition of MST1/2, an LTB4 receptor 1 (BLT1) antagonist was used, and it dramatically improved cardiac repair in mice treated with XMU-MP-1 or with macrophage-specific *Mst1/2* knockout. In the current study, we present a new therapeutic concept for the treatment of MI by combining an MST1/2 inhibitor tissue-repair drug and a BLT1 antagonist.

METHODS

Data Availability.

All supporting data are available within the article and its Online Supplementary Materials. Detailed descriptions of experimental methods of the current study are provided in the Online Supplementary Materials.

RESULTS

Mst1/2 conditional knockout exacerbates cardiac dysfunction following MI in mice.

To demonstrate the role of macrophage Mst1/2 in cardiac repair post-MI, we performed permanent ligation of the left anterior descending coronary artery in mice to mimic MI in humans. We examined the expression of endogenous Mst1 in cardiac macrophages of wild-type mice on Day 1, 3 and 7 after MI, respectively. Compared to Day 0, the expression of Mst1 decreased in the first 3 days after MI, reaching the lowest value on Day 1, and increased moderately on Day 7, suggesting the role of Mst1 in cardiac inflammatory response in MI (Fig. 1A and Online Figure IA). However, total and phosphorylated YAP protein level was continuously increased from Day 1 to Day 7 after MI compared to Day 0 (Online Figure IA), suggesting that the regulation of YAP in macrophages by inflammatory stimulus might be in a transcriptional manner and independent of canonical Hippo pathway (kinase Mst1/2). Next, we crossed *Mst1/2*$^{flox/flox}$ mice with *LysMCre* mice to delete the target genes in myeloid cells, such as monocytes, macrophages and neutrophils. To determine the effects of macrophage MST1/2 on cardiac function following MI, we measured the left ventricular end-diastolic volume (LVEDV), left ventricular end-systolic volume (LVESV), ejection fraction (EF), and fractional shortening (FS) by echocardiography. The baseline values of these parameters were similar in *LysMCre-Mst1/2*$^{flox/flox}$ and *Mst1/2*$^{flox/flox}$ mice on Day 0 (before surgery) (Fig. 1B and 1C). On Day 3 and 7 post-MI, LVEDV and LVESV were significantly higher, and EF and FS were lower, in *LysMCre-Mst1/2*$^{flox/flox}$ mice than in *Mst1/2*$^{flox/flox}$ mice. However, on days 0, 3, and 7, no differences were observed between the two strains in the numbers of infiltrated macrophages, monocytes, and neutrophils in the mice hearts (Fig. 1D and Online Figure IB). To exclude the effect of neutrophils, we crossed *Mst1/2*$^{flox/flox}$ mice with *Cx3cr1Cre* mice, expressing in monocytes, macrophages and microglial cells. Consistently, *Cx3cr1Cre-Mst1/2*$^{flox/flox}$ mice had similar phenotypes as *LysMCre-Mst1/2*$^{flox/flox}$ mice after MI (Online Figure IC-F).

Macrophages in MI are heterogeneous [25], so we applied unbiased single-cell RNA sequencing to identify immune-cell populations in the hearts of *LysMCre-Mst1/2*$^{flox/flox}$ and *Mst1/2*$^{flox/flox}$ mice on Day 3 post-MI. After extensive filtration and quality control, 4014 digested single cells were subjected to subsequent analyses. To classify major immune-cell types in hearts undergoing remodeling, we performed cluster analysis and defined seven major clusters, including three subtypes of macrophages (MP1-3), two subtypes of B cells (B1 and B2), granulocytes (GR), and T cells (T), bases on specific molecular markers (Fig. 1E). Each cell cluster expressed distinct signature genes, and contained cells

from two individuals, suggesting reproducibility (Online Figure IIA-B). To characterize immune-cell clusters in MI, we evaluated gene-expression differences among the cells in macrophage, B cell and granulocyte clusters (Fig. 1F and Online Figure IIC). Among the three identified macrophage subtypes, MP1 cells highly expressed the proinflammatory genes *Ccl4*, *Ccl2*, and *Spp1*. In contrast, MP2 cells had a high expression of anti-inflammatory genes such as *Cd163*, *Cbr2*, and *Rgs10*. MP3 cells had mixed properties, with the expression of anti-inflammatory (*Slpi* and *Arg1*) and pro-angiogenic (*Cxcl2*) genes (Fig. 1F). Next, we characterized the effects of *Mst1/2* knockout on the proportions of macrophage subtypes. MP1 was the most prevalent macrophage subtype in each mouse strain, and the proportion of MP1 in *LysMCre-Mst1/2$^{flox/flox}$* mice was higher than in *Mst1/2$^{flox/flox}$* mice (77.8% versus 59.5%) (Fig. 1G). In contrast, both MP2 (28.93% versus 15.28%) and MP3 (11.57% versus 6.94%) showed a lower proportion in *LysMCre- Mst1/2$^{flox/flox}$* mice (Fig. 1G). Furthermore, we found that *LysMCre-Mst1/2$^{flox/flox}$* mice had significantly higher expression of MP1 marker genes (*Ccl4*, *Ccl2*, and *Spp1*) and lower expression of MP2 and MP3 marker genes (*Cd163*, *Slpi*, and *Cxcl2*) than *Mst1/2$^{flox/flox}$* mice in heart tissue on Day 3 post-MI (Fig. 1H). In line to single-cell analysis and real-time PCR assays, Spp1 fluorescence intensity in CD68 positive area on the heart sections was significantly higher in *LysMCre-Mst1/2$^{flox/flox}$* than *Mst1/2$^{flox/flox}$* mice, while Cd163 and Arg1 were reduced (Online Figure IID-F). Taken together, these findings suggested that MST1/2 knockout promoted macrophage subtype switching and impaired inflammation resolution in the mice hearts post-MI.

MST1 deficiency induces LTB4 production in macrophages.

The basal expression of inflammatory factors is not affected by MST1 deficiency in macrophages cultured for a short time [26]. Therefore, we determine whether MST1 exerts paracrine proinflammatory actions in MI. We collected conditioned media (CM) from the culture of peritoneal macrophages derived from *Mst1$^{-/-}$* mice or their littermate *Mst1$^{+/+}$* controls, and used them to treat wild-type (WT) macrophages. Expression of proinflammatory genes (*Ccl4* and *Ccl2*) was significantly higher in WT macrophages treated with CM from *Mst1$^{-/-}$* macrophages than those treated with CM from *Mst1$^{+/+}$* macrophages (Fig. 2A). We pretreated the CM with trypsin or dextran-coated charcoal (DCC) to remove proteins or small molecules, respectively [27]. Our result showed that the proinflammatory effect of CM from MST1-deficient macrophages was eliminated by DCC treatment but not by trypsin, suggesting the involvement of small molecules rather than proteins or large peptides. Notably, eicosanoids are small lipid molecules that play critical roles in the inflammation and resolution process in macrophages [28, 29]. To identify the proinflammatory component in the CM of MST1-deficient macrophages, we analyzed the lipidomic profile of arachidonic acid, eicosapentaenoic acid, and docosapentaenoic acid metabolites by highly specific liquid chromatography-tandem mass spectrometry (LC-MS/MS). An orthogonal partial least squares discriminant analysis (PLS-DA) model that was built based on the measured metabolites demonstrated robust separation of the two groups (*Mst1$^{-/-}$* and *Mst1$^{+/+}$* CM), indicating that MST1-deficient macrophages had a distinct metabolomic signature from *Mst1$^{+/+}$* macrophages (Fig. 2B). Heatmap analysis of the levels of 56 metabolites revealed notable differences between *Mst1$^{-/-}$* and *Mst1$^{+/+}$* CM (Fig. 2C). Levels of LTB4 showed the greatest difference between the groups by variable importance in projection analysis and fold-difference in concentration (Fig. 2D-E). Production of three

other 5-LOX-derived leukotrienes (lipoxin A4, 4-hydroxydocosahexanoic acid, and 5-hydroxyeicosatetraenoic acid) was also significantly higher in CM of *Mst1*-deficient macrophages than in $Mst1^{+/+}$ CM, but to a lesser extent than LTB4, whereas levels of leukotriene E4 (LTE4), leukotriene C4 (LTC4), resolvin E1, resolvin D1, and resolvin D2 did not show a significant difference (Fig. 2F). Consistently, cardiac LTB4 levels were also significantly higher in *LysMCre-Mst1/2*$^{flox/flox}$ or in *Cx3cr1Cre-Mst1/2*$^{flox/flox}$ mice on Day 3 post-MI than in *Mst1/2*$^{flox/flox}$ mice (Fig. 2G and Online Figure IIIA). We also isolated macrophages and neutrophils from the hearts of *Mst1/2*$^{flox/flox}$ and *LysMCre-Mst1/2*$^{flox/flox}$ mice on Day 3 after MI and measured LTB4 production. The LTB4 production of cardiac neutrophils was comparable between *Mst1/2*$^{flox/flox}$ and *LysMCre-Mst1/2*$^{flox/flox}$ mice. In contrast, the LTB4 production of cardiac macrophages was dramatically increased in *LysMCre-Mst1/2*$^{flox/flox}$ mice compared to *Mst1/2*$^{flox/flox}$ mice (Online Figure IIIB-C). These data suggested that Mst1/2-induced LTB4 production predominantly occurs in macrophages rather than neutrophils. Furthermore, we isolated peritoneal macrophages from *WT*, *Mst1*$^{-/-}$, and *Mst1-YAP*^{DKO} mice. Consistently, we found LTB4 production was higher in macrophages from *Mst1*$^{-/-}$ mice than that of *WT* mice (Online Figure IIID). Notably, LTB4 production was similar in macrophages from *Mst1*$^{-/-}$ and *Mst1-YAP*^{DKO} mice (Online Figure IIID), suggesting that YAP might be dispensable in Mst1 deficiency-induced LTB4 production in macrophages. Furthermore, the levels of LTB4 in plasma from patients with ST-elevation MI (STEMI) were significantly higher than plasma from control individuals (Fig. 2H and Online Table I), indicating an association between LTB4 and MI injury. In summary, our results suggested that proinflammatory effects of MST1 deficiency in macrophages were mediated by 5-LOX-derived LTB4 synthesis in a paracrine manner.

The interaction between 5-LOX and FLAP is disrupted by MST1-mediated 5-LOX phosphorylation at T218.

Following our observation that MST1 deficiency promoted the production of metabolites derived from 5-LOX, we further investigated the regulation of 5-LOX. We found that loss of MST1 in macrophages did not alter mRNA or protein levels of 5-LOX in those cells (Fig. 3A-B). To determine whether the serine/threonine kinase MST1 could regulate 5-LOX post-translationally, we overexpressed Myc-tagged MST1 and Flag-tagged 5-LOX in HEK293T cells and found that immunoprecipitation with anti-Flag antibodies pulled down Myc-tagged MST1 (Fig. 3C). The amino-terminal β-sandwich (PLAT) of 5-LOX mediates protein–protein and protein–lipid interactions [30, 31]; therefore, we deleted the PLAT domain and tagged the remaining protein with Flag, to give 5-LOX$^{\Delta PLAT}$. Full-length 5-LOX, but not 5-LOX$^{\Delta PLAT}$, interacted with MST1 (Fig. 3D), indicating that MST1 bound to 5-LOX at the PLAT domain.

Previous studies showed that phosphorylation of S271 inhibit the nuclear export of 5-LOX, whereas phosphorylation of S523 inhibits its nuclear import [32, 33]. However, we found that phosphorylation of S271 and S523 was not influenced by MST1 overexpression (Online Figure IVA). To identify the MST1 phosphorylation sites on 5-LOX, we performed LC-MS/MS on Flag-5-LOX expressed in HEK293T cells with Myc-MST1, and found the three most likely sites, which were located at S216, T218, and T428 (Fig.

3E). We then generated three phospho-refractory variants of 5-LOX with serine/threonine residues replaced by alanine (S216A, T218A and T428A), and found that only T218A diminished MST1-mediated 5-LOX phosphorylation (Fig. 3F). A polyclonal antibody against 5-LOX phosphorylated at T218 was generated and verified that T218 was the specific Mst1-targeted phosphorylation site on 5-LOX (Fig. 3F and Online Figure IVB). Furthermore, we expressed Flag-5-LOX in HEK293T cells with and without MST1, then immunoprecipitated the lipoxygenase and assessed its phosphorylation by immunoblot analysis with antibody against 5-LOX phosphorylated at T218. Co-expression of MST1 enhanced dose-dependently phosphorylation of 5-LOX^{T218}, whereas a lower level of phosphorylation was observed with overexpression of a Myc-tagged kinase-deficient variant of MST1 (MST1^{K59R}) (Fig. 3G-H) [26]. In contrast, the phosphorylation of 5-LOX^{T218} was significantly decreased in peritoneal macrophages from *LysMCreMst1/2$^{flox/flox}$* knockout mice than *Mst1/2$^{flox/flox}$* mice (Online Figure IVC). To explore whether MST1 directly phosphorylates 5-LOX ^{T218}, we performed an in vitro kinase assay with purified recombinant proteins of MST1, 5-LOX and 5-LOX ^{T218A}. Purified 5-LOX did not show phosphorylation in the absence of MST1 but did show phosphorylation when wild-type MST1 was added. However, purified 5-LOX ^{T218A} showed no response to wild-type MST1 (Online Figure IVD). Next, we constructed *5-LOX$^{T218Aflox/+}$* mice using conventional CRISPR/Cas9 approaches (Online Figure IVE). To confirm the findings in HEK293T cells, peritoneal macrophages from *5-LOX$^{T218A-flox/+}$* and *LysMCre-5-LOX$^{T218A-flox/+}$* mice were isolated and transfected with Myc-MST1. The phosphorylation of 5-LOX^{T218} by immunoblot analysis was increased by MST1 overexpression in macrophages from *5-LOX$^{T218A-flox/+}$* mice. Heterozygous T218A mutation dramatically reduced phosphorylated 5-LOX^{T218} in macrophages, which showed moderate response to MST1 overexpression (Online Figure IVF). Taken together, our results demonstrated that 5-LOX bound MST1 through the PLAT domain, and was phosphorylated by MST1 at T218.

To determine whether phosphorylation might regulate the 5-LOX activity, plasmids directing expression of 5-LOX or 5-LOX^{T218A} were transfected into HEK293T cells. The catalytic interaction between 5-LOX and FLAP does not occur in homogenates [34], so intact cells showed higher LTB4 production (Fig. 4A). HEK293T cells expressing 5-LOX had comparable LTB4 production to those expressing 5-LOX^{T218A}, both in intact cells and homogenates (Fig. 4A). LTB4 production was significantly higher in intact cells co-expressing FLAP and either 5-LOX or 5-LOX^{T218A} than in the absence of FLAP expression, and LTB4 levels were highest in cells co-expressing FLAP and 5-LOX^{T218A}. Co-expression of FLAP did not affect LTB4 production in cell homogenates (Fig. 4A). In addition, no significant differences in the production of LTC4 or leukotriene X4 (LTX4) were observed among these groups in intact cells or homogenates (Online Figure VA).

LTB4 biosynthesis requires subcellular redistribution of 5-LOX to nuclear-membrane-embedded FLAP for effective AA transfer [35], so we next determined the effects of MST1 on 5-LOX subcellular localization. We transfected HEK293T cells with plasmids directing expression of 5-LOX and FLAP and found that resting cells exhibited homogenous intranuclear staining of 5-LOX (Fig. 4B), which are consistent with the previous studies [34, 36, 37]. Upon treatment with a Ca^{2+}-ionophore (A23187), 5-LOX rapidly translocated to the nuclear membrane and co-localized with FLAP. Translocation and

co-localization were prevented by co-expression of MST1, but not by MST1^{K59R}. MST1 did not prevent redistribution of 5-LOX^{T218A} in response to A23187. The results of proximity ligation assays confirmed that co-localization of 5-LOX with FLAP occurred on A23187 treatment in the absence of MST1 or in the presence of MST1^{K59R}, or with the combination of 5-LOX^{T218A} and MST1, but not with the combination of 5-LOX and MST1 (Fig. 4C). Furthermore, monocytes from *LysMCre-Mst1/2$^{flox/flox}$* conditional-knockout mice showed greater levels of A23187-stimulated interactions of 5-LOX with FLAP than cells from *Mst1/2$^{flox/flox}$* mice (Fig. 4D). Accordingly, co-expression of MST1, but not of MST1^{K59R}, suppressed LTB4 production in intact HEK293T cells expressing 5-LOX and FLAP, whereas live cells expressing 5-LOX^{T218A}, FLAP, and MST1 maintained high levels of LTB4 production (Fig. 4E). LTB4 production levels in cell homogenates were similar in these four groups. Consistently, the production levels of LTC4 and LTX4 did not differ significantly among these groups in intact cells or homogenates (Online Figure IVB). Furthermore, peritoneal macrophages from *5-LOX$^{T218A\text{-}flox/+}$* and *LysMCre-5-LOX$^{T218A\text{-}flox/+}$* mice were electroporated with Myc-tagged MST1 plasmids, and then the production levels of LTB4 were measured. LTB4 production was significantly higher in intact macrophages in *LysMCre-5-LOX$^{T218A\text{-}flox/+}$* mice compare to *5-LOX$^{T218A\text{-}flox/+}$* mice. MST1 overexpression suppressed LTB4 production in intact macrophages from *5-LOX$^{T218A\text{-}flox/+}$* mice but to a much lesser extent in cells from *LysMCre-5-LOX$^{T218A\text{-}flox/+}$* mice. However, LTB4 production levels in cell homogenates were similar in these four groups (Online Figure IVC).

These findings indicated that MST1-mediated phosphorylation of 5-LOX at T218 blocked the translocation of 5-LOX and its physical interaction with FLAP to inhibit LTB4 production and did not directly affect the enzymatic activity of 5-LOX.

The LTB4–BLT1 axis contributes to MST1-deficiency-induced inflammatory responses in macrophages.

To investigate whether the LTB4-activated BLT1 pathway participated in *Mst1*-deficiency-induced macrophage subtype switching, WT macrophages were pretreated with BLT1 antagonist (CP105696) or with vehicle only, and then treated with or without LTB4 in the medium. In the absence of CP105696 pretreatment, mRNA levels corresponding to the proinflammatory MP1 markers *Ccl4*, *Ccl2*, and *Spp1* were significantly enhanced by LTB4 treatment, whereas those of the anti-inflammatory and angiogenic MP2/3 markers *Cd163*, *Slpi*, and *Cxcl2* were significantly downregulated (Fig. 5A). CP105696 pretreatment did not significantly affect marker expression relative to vehicle-only pretreatment, but it substantially inhibited upregulation of MP1 marker expression and downregulation of MP2/3 marker expression induced by LTB4. We also determined the expression of proteins from classic cellular signaling pathways involved in switching macrophage subtype, and found that LTB4 significantly induced phosphorylation of JNK, ERK1/2, and p65 (but not p38), relative to levels in vehicle-only controls (Fig. 5B-C). With CP105696 pretreatment, no significant differences were observed in levels of phosphorylation, with or without LTB4. Similarly, CM from MST1-deficient macrophages induced WT-macrophage subtype switching (demonstrated by MP1–3 gene-expression profiles and protein phosphorylation levels), this effect was blocked by CP105696 pretreatment (Fig. 5D-F). Our results

suggested that LTB4 and BLT1 participated in *Mst1*-deficiency-induced macrophage subtype switching in a paracrine manner through JNK/ERK1/2/ NF-κB pathways.

Treatment with a BLT1 antagonist improves cardiac repair in Mst1/2-deficient mice post-MI.

To determine the effect of CP105696 in cardiac repair in vivo, and to demonstrate the clinical relevance of our findings, we treated *Mst1/2*$^{flox/flox}$ and *LysMCre-Mst1/2*$^{flox/flox}$ mice with CP105696 on 7 days pre- and 28 days post-MI. Echocardiographic measurements of LVEDV, LVESV, EF, FS and cardiac output (CO) were measured on Day 0, 1, 3, 7, and 28 after MI (Fig. 6A-B and Online Figure VIA). These parameters were comparable on Day 1 among all groups. Compared with *Mst1/2*$^{flox/flox}$ mice, *LysMCre-Mst1/2*$^{flox/flox}$ mice had impaired cardiac function post MI, as evidenced by higher LVEDV and LVESV and lower EF and FS values, which were rescued by CP105696 treatment (Fig. 6A-B). The increased ratios of heart-to-body weight and lung-to-body weight and mortalities in *LysMCre-Mst1/2*$^{flox/flox}$ mice were reversed by CP105696 treatment (Fig. 6C-D). In vehicle-treated mice, the fibrotic area was greater in *LysMCre-Mst1/2*$^{flox/flox}$ mice than *Mst1/2*$^{flox/flox}$ mice (Fig. 6E-F) on Day 28 post MI. Treatment of *LysMCre-Mst1/2*$^{flox/flox}$ mice with CP105696 reduced the fibrotic area compared with vehicle-treated mice. Administration of CP105696 in *Mst1/2*$^{flox/flox}$ mice had a similar trend but to a lesser extent.

Clearance of apoptotic cells by macrophages and angiogenesis are important for inflammation resolution and cardiac repair post-MI [38, 39]. We found that post-MI, protein levels of proapoptotic regulator Bax and cleaved caspase-3 were higher and antiapoptotic Bcl-2 levels were lower in the left ventricles of vehicle-treated *LysMCre-Mst1/2*$^{flox/flox}$ mice than in vehicle-treated *Mst1/2*$^{flox/flox}$ mice (Online Figure VIB-C). We did not found any differences between the protein levels in vehicle-treated *Mst1/2*$^{flox/flox}$ mice and CP105696-treated *LysMCre-Mst1/2*$^{flox/flox}$ mice. Moreover, CP105696 further suppressed the protein levels of Bax and enhanced the levels of Bcl2 in *Mst1/2*$^{flox/flox}$ mice than vehicle-treated *Mst1/2*$^{flox/flox}$ mice. Based on these findings, we performed terminal-deoxynucleotidyltransferase-mediated dUTP nick-end labeling (TUNEL) immunofluorescence staining of left ventricle sections. We found a higher proportion of cardiac apoptotic cells in border areas of hearts in vehicle-treated *LysMCre-Mst1/2*$^{flox/flox}$ mice than in vehicle-treated *Mst1/2*$^{flox/flox}$ mice, but no differences between these values in CP105696-treated *LysMCre-Mst1/2*$^{flox/flox}$ mice and vehicle-treated *Mst1/2*$^{flox/flox}$ mice (Online Figure VID-E). In addition, a lower intensity of CD31 was observed in border areas of hearts in vehicle-treated *LysMCre-Mst1/2*$^{flox/flox}$ mice than in vehicle-treated *Mst1/2*$^{flox/flox}$ mice, but no differences between these values in CP105696-treated LysMCre-*Mst1/2*$^{flox/flox}$ mice and vehicle-treated *Mst1/2*$^{flox/flox}$ mice (Fig. 6G-H). Similarly, CP105696 treatment prevented the post-MI elevation of expression of proinflammatory genes (*Tnfa*, *Il1b*, *Ccl4*, *Ccl2*, and *Spp1*) and reduction of expression of anti-inflammatory genes (*Slpi* and *Arg1*) and proangiogenic genes (*Cxcl2, Fgf2,* and *Vegfa*) in the hearts of *LysMCre-Mst1/2*$^{flox/flox}$, which were also changed in *Mst1/2*$^{flox/flox}$ mice but to a much lesser extent (Fig. 6I). In addition, cardiac LTB4 levels were significantly higher in vehicle-treated *LysMCre-Mst1/2*$^{flox/flox}$ mice than in vehicle-treated *Mst1/2*$^{flox/flox}$ mice, and were also high in CP105696-treated *LysMCre-Mst1/2*$^{flox/flox}$ mice (Online Figure VIF).

XMU-MP-1 is a novel inhibitor of MST1/2 kinase that promotes liver repair and improves cardiac function following pressure overload in mice [40, 41]. Considering the proinflammatory effect of MST1 deficiency in macrophages, we imagined a new therapeutic concept that a combination of XMU-MP-1 and a BLT1 antagonist might synergistically benefit cardiac repair post-MI. We then assessed the impact of this therapeutic strategy on cardiac function in mice after MI injury. The four groups of mice have a similar cardiac function on Day 1 after MI. XMU-MP-1 did not have a strong effect as a tissue repair drug by Day 28 post-MI. However, mice with the XMU-MP-1 in combination with CP105696 treatment had lower LVEDV and LVESV and higher EF, FS and CO than mice with single-drug or vehicle treatments starting from Day 3 (Fig. 7A-B and Online Figure VIIA). The ratios of heart and lung to body weight and mortalities were lower in mice with combination treatment compared to other groups (Fig. 7C-D). WT mice treated with XMU-MP-1 had significantly higher fibrotic and lower CD31 positive areas than vehicle-treated mice on Day 28 post-MI (Fig. 7E-H). However, mice treated with XMU-MP-1 in combination with CP105696 had significantly lower fibrotic and increased CD31 positive area than mice treated with vehicle or single-drug. In mice treated with XMU-MP-1, cardiac expression of proinflammatory genes (*Tnfa*, *Il1b*, *Ccl4*, *Ccl2*, and *Spp1*) was significantly higher, and expression of anti-inflammatory genes (*Slpi* and *Arg1*) and proangiogenic genes (*Cxcl2, Fgf2,* and *Vegfa*) were significantly lower than in mice treated with vehicle or the combination therapy (Fig. 7G-I). Accordingly, this combination approach significantly attenuated cardiac levels of apoptotic markers (Online Figure VIIB-C), and reduced numbers of TUNEL-positive cells in border areas of the heart (Online Figure VIID-E) than the single-drug or vehicle treatments. The LTB4 levels in hearts were increased by XMU-MP-1, regardless of BLT1 activity (Online Figure VIIF). Together, the combined effect of XMU-MP-1 and CP105696 significantly improved cardiac repair after MI in mice, suggesting a promising new therapeutic strategy for MI.

DISCUSSION

The Hippo pathway has an important role in stem cell self-renewal, tissue regeneration and angiogenesis, contributing to post-MI cardiac repair. As a small molecule that targets the Hippo-pathway kinases MST1/2, XMU-MP-1 has attracted attention as a promising therapeutic candidate for regenerative medicine. However, the extensive involvement of MST1/2 in immune regulation may restrict the use of XMU-MP-1 in tissue repair or tissue remodeling, which is tightly orchestrated by immune cells. Dysregulation of immune pathways, impaired spatial containment of the inflammatory response, and overactive fibrosis may cause adverse remodeling in patients with MI, leading to heart failure. Here, we demonstrated that macrophage-specific deficiency of MST1/2 aggravated MI injury in mice via induction of LTB4 production and promotion of macrophage subtype switching to a proinflammatory profile in a paracrine manner. Moreover, we identified 5-LOX as a substrate of MST1 kinase and assessed a therapeutic combination with the potential to overcome the limitations of XMU-MP-1 and enhance cardiac repair by global MST1/2 inhibition in the setting of MI.

The most significant finding of our study was the association of the Hippo pathway with the production of lipid mediators. Although the kinases LATS1 and LATS2 are the classic downstream effectors of the Hippo pathway, several other factors (including FOXO1, IRAK1, STAT5, and NRF2) have been shown to predominantly mediate MST1 functions as its catalytic substrates in immune cells in response to pathogens and specific cytokines [26, 42-44]. Here, we identified a conserved MST1 phosphorylation site at a threonine residue (T218) in 5-LOX, which contributes to determining the production pattern of arachidonic-acid-derived lipid mediators in macrophages. As a key enzyme in initiating leukotriene synthesis from arachidonic acid, 5-LOX targets the nuclear membranes to convert arachidonic acid to 5-hydroperoxyeicosatetraenoic acid and leukotriene A4, in a process that requires the integral nuclear envelope protein FLAP [45, 46]. Localization of 5-LOX to the inner or outer nuclear membrane determines the relative production of LTB4 and LTC4 [47, 48], and phosphorylation of 5-LOX at S271 or S523 affects its subcellular distribution [32, 33, 49]. We found that a variant of 5-LOX with a T218A substitution had an identical nuclear accumulation profile to WT 5-LOX in the presence of MST1 co-expression in HEK293 cells. However, treatment with a calcium ionophore did not change the distribution of WT 5-LOX, whereas the 5-LOX^{T218A} translocated to the nuclear membrane and co-localized with FLAP, resulting in high levels of LTB4 production. These findings suggest that in HEK293 cells, the preferential localization of 5-LOX^{T218A} at the inner nuclear membrane was independent of nuclear–cytoplasmic shuttling, and the MST1-catalysed 5-LOX phosphorylation event likely occurred in the nucleus and inhibited LTB4 production. According to these observations and the known cellular distributions of the molecular machinery for LTB4 synthesis [50], we postulate that T218 phosphorylation may also occur in the nuclei of macrophages, especially when the nuclear export signal of MST1 is inactivated in certain contexts. In support of this hypothesis, similar scenarios have been proposed for the nuclear kinase activity of MST1 towards histone H2B [15, 51]. The MST1 deficiency also mildly elevated levels of other leukotrienes produced by 5-LOX in the cytoplasmic region of macrophages, so it is possible that MST1-promoted 5-LOX phosphorylation also occurs in the cytoplasm. Using *Mst1-YAP*^{DKO} mice, we found that YAP was dispensable in Mst1 deficiency-induced LTB4 production in macrophages, suggesting that macrophage YAP and Mst1 contribute to cardiac repair post MI independently[13].

Using MST1/2 inhibition as a therapeutic strategy for recovery from MI, we identified a critical role for the excessive production of proinflammatory LTB4. Leukotrienes have important roles in the control of local inflammation in MI. Support for this notion comes from genetic deletion of 12/15 lipoxygenase, which promotes effective resolution of inflammation following MI [52]. Here, we observed approximately two-fold increases in *Ccl4* and *Ccl2* in WT macrophages incubated with CM from MST1-deficient macrophages (relative to treatment with *Mst1*$^{+/+}$ CM), and identified LTB4 as a primary proinflammatory lipid mediator in the CM. LTB4 is known to be involved in neutrophil recruitment [53], we observed similar ratios of cardiac neutrophils to total white blood cells in *LysMCre*-mediated *Mst1/2*-knockout mice and *Mst1/2*$^{flox/flox}$ mice post-MI, which might be explained by an MST1-deficiency-induced impairment of neutrophil transmigration activity [54]. Inhibition of BLT1 with CP105696 improved the cardiac dysfunction in mice with genetic or pharmacological inhibition of Mst1/2 after MI, and reduced scar size, cardiac inflammation gene expression and apoptosis-associated protein levels in the hearts of *Mst1/2*$^{flox/flox}$ or also vehicle-treated WT mice. These findings indicated that the pro-inflammatory effect of LTB4 is not

only generated in the specific circumstance of treatment with Mst1/2 inhibition post-MI, but also a part of the physiological response to untreated MI. Notably, we found that plasma LTB4 concentrations were significantly higher in patients with STEMI, in *LysMCre-Mst1/2*$^{flox/flox}$ mice, and MST1/2-inhibitor-treated mice than their respective controls. Our findings indicate that LTB4 is a potential marker for diagnosis and prognostication for cardiac repair post-MI. Further investigations with clinical surveillance to adequately assess the reliability of LTB4 in clinical decision-making are needed.

Two G-protein-coupled receptors exist for LTB4, BLT1 and BLT2. BLT1 is mainly expressed in leukocytes and exhibits selective specificity for LTB4, whereas BLT2 has ubiquitous expression and responds to other 5-LOX-produced leukotrienes. The LTB4–BLT1 axis has an important role in chronic inflammatory processes, such as atherosclerosis and insulin resistance, through activation of the expression of JNK-induced inflammatory factors in macrophages [55]. We, therefore, investigated the effects of CP105696, a highly selective antagonist of BLT1. With single-cell RNA sequencing, we found higher proportions of macrophages highly expressing *Ccl4* and *Ccl2* and lower proportions highly expressing *Cd163* or angiogenic factor *Cxcl2* in *LysMCre-Mst1/2*$^{flox/flox}$ mice than in *Mst1/2*$^{flox/flox}$ mice, suggesting proinflammatory and anti-angiogenic effects of LTB4 for macrophages. In several different assays both in vitro and in vivo, similar effects of LTB4 treatment and MST1/2 deficiency post-MI were prevented by treatment with the BLT1 antagonist. Thus, we proposed and provided supporting evidence for the use of a combination of BLT1 antagonist and MST1/2 inhibitor to achieve a synergistic effect and accelerate the cardiac healing process post-MI. Also, the strong effect of CP treatment suggests the importance of inflammation in cardiac repair after MI.

In summary, we determined that the MST1–5-LOX–LTB4–BLT1 axis is a key regulator of cardiac repair post-MI, and LTB4 should be evaluated as a diagnostic and prognostic marker for MI. We have also developed a therapeutic combination of the MST1/2 inhibitor and tissue-repair drug XMU-MP-1 with the BLT1 antagonist CP105696, which can overcome negative inflammatory consequences of treatment with XMU-MP-1 alone and thus ameliorate MI injury and prevent heart failure.

SOURCES OF FUNDING

This work was supported by the National Natural Science Foundation of China Grants (81925003), National Key Research and Development Program of China Grants (2019YFA0802502), and Tianjin Natural Science Foundation of China (17JCJQJC45700, 17JCJQJC46100 and 19JCZDJC64800). H.J. was supported by Young Elite Scientists Sponsorship Program by CAST (2019QNRC001).

DISCLOSURES

None.

SUPPLEMENTAL MATERIALS

Expanded Materials & Methods

Online Figures I – VII

Online Tables I- I I

References56-69

REFERENCES

1. Broughton KM, Wang BJ, Firouzi F, Khalafalla F, Dimmeler S, Fernandez-Aviles F and Sussman MA. Mechanisms of Cardiac Repair and Regeneration. *Circ Res*. 2018;122:1151-1163.
2. Shirazi LF, Bissett J, Romeo F and Mehta JL. Role of Inflammation in Heart Failure. *Curr Atheroscler Rep*. 2017;19:27.
3. Basil MC and Levy BD. Specialized pro-resolving mediators: endogenous regulators of infection and inflammation. *Nat Rev Immunol*. 2016;16:51-67.
4. Fredman G, Hellmann J, Proto JD, Kuriakose G, Colas RA, Dorweiler B, Connolly ES, Solomon R, Jones DM, Heyer EJ, Spite M and Tabas I. An imbalance between specialized pro-resolving lipid mediators and pro-inflammatory leukotrienes promotes instability of atherosclerotic plaques. *Nat Commun*. 2016;7:12859.
5. Zhang XJ, Cheng X, Yan ZZ, Fang J, Wang X, Wang W, Liu ZY, Shen LJ, Zhang P, Wang PX, Liao R, Ji YX, Wang JY, Tian S, Zhu XY, Zhang Y, Tian RF, Wang L, Ma XL, Huang Z, She ZG and Li H. An ALOX12-12-HETE-GPR31 signaling axis is a key mediator of hepatic ischemia-reperfusion injury. *Nat Med*. 2018;24:73-83.
6. Sharma JN and Mohammed LA. The role of leukotrienes in the pathophysiology of inflammatory disorders: is there a case for revisiting leukotrienes as therapeutic targets? *Inflammopharmacology*. 2006;14:10-6.
7. Qiu H, Gabrielsen A, Agardh HE, Wan M, Wetterholm A, Wong CH, Hedin U, Swedenborg J, Hansson GK, Samuelsson B, Paulsson-Berne G and Haeggstrom JZ. Expression of 5-lipoxygenase and leukotriene A4 hydrolase in human atherosclerotic lesions correlates with symptoms of plaque instability. *Proc Natl Acad Sci U S A*. 2006;103:8161-6.
8. Dwyer JH, Allayee H, Dwyer KM, Fan J, Wu H, Mar R, Lusis AJ and Mehrabian M. Arachidonate 5-lipoxygenase promoter genotype, dietary arachidonic acid, and atherosclerosis. *N Engl J Med*. 2004;350:29-37.
9. Spanbroek R, Grabner R, Lotzer K, Hildner M, Urbach A, Ruhling K, Moos MP, Kaiser B, Cohnert TU, Wahlers T, Zieske A, Plenz G, Robenek H, Salbach P, Kuhn H, Radmark O, Samuelsson B and Habenicht AJ. Expanding expression of the 5-lipoxygenase pathway within the arterial wall during human atherogenesis. *Proc Natl Acad Sci U S A*. 2003;100:1238-43.
10. Zhao B, Tumaneng K and Guan KL. The Hippo pathway in organ size control, tissue regeneration and stem cell self-renewal. *Nat Cell Biol*. 2011;13:877-83.
11. Halder G and Johnson RL. Hippo signaling: growth control and beyond. *Development*. 2011;138:9-22.

12. Harvey KF, Pfleger CM and Hariharan IK. The Drosophila Mst ortholog, hippo, restricts growth and cell proliferation and promotes apoptosis. *Cell*. 2003;114:457-67.
13. Mia MM, Cibi DM, Abdul Ghani SAB, Song W, Tee N, Ghosh S, Mao J, Olson EN and Singh MK. YAP/TAZ deficiency reprograms macrophage phenotype and improves infarct healing and cardiac function after myocardial infarction. *PLoS Biol*. 2020;18:e3000941.
14. Qin F, Tian J, Zhou D and Chen L. Mst1 and Mst2 kinases: regulations and diseases. *Cell Biosci*. 2013;3:31.
15. Ura S, Masuyama N, Graves JD and Gotoh Y. Caspase cleavage of MST1 promotes nuclear translocation and chromatin condensation. *Proc Natl Acad Sci U S A*. 2001;98:10148-53.
16. Yamamoto S, Yang G, Zablocki D, Liu J, Hong C, Kim SJ, Soler S, Odashima M, Thaisz J, Yehia G, Molina CA, Yatani A, Vatner DE, Vatner SF and Sadoshima J. Activation of Mst1 causes dilated cardiomyopathy by stimulating apoptosis without compensatory ventricular myocyte hypertrophy. *J Clin Invest*. 2003;111:1463-74.
17. Odashima M, Usui S, Takagi H, Hong C, Liu J, Yokota M and Sadoshima J. Inhibition of endogenous Mst1 prevents apoptosis and cardiac dysfunction without affecting cardiac hypertrophy after myocardial infarction. *Circ Res*. 2007;100:1344-52.
18. He J, Bao Q, Zhang Y, Liu M, Lv H, Liu Y, Yao L, Li B, Zhang C, He S, Zhai G, Zhu Y, Liu X, Zhang K, Wang XJ, Zou MH, Zhu Y and Ai D. Yes-Associated Protein Promotes Angiogenesis via Signal Transducer and Activator of Transcription 3 in Endothelial Cells. *Circ Res*. 2018;122:591-605.
19. Xin M, Kim Y, Sutherland LB, Murakami M, Qi X, McAnally J, Porrello ER, Mahmoud AI, Tan W, Shelton JM, Richardson JA, Sadek HA, Bassel-Duby R and Olson EN. Hippo pathway effector Yap promotes cardiac regeneration. *Proc Natl Acad Sci U S A*. 2013;110:13839-44.
20. Heallen T, Morikawa Y, Leach J, Tao G, Willerson JT, Johnson RL and Martin JF. Hippo signaling impedes adult heart regeneration. *Development*. 2013;140:4683-90.
21. Leach JP, Heallen T, Zhang M, Rahmani M, Morikawa Y, Hill MC, Segura A, Willerson JT and Martin JF. Hippo pathway deficiency reverses systolic heart failure after infarction. *Nature*. 2017;550:260-264.
22. Abdollahpour H, Appaswamy G, Kotlarz D, Diestelhorst J, Beier R, Schaffer AA, Gertz EM, Schambach A, Kreipe HH, Pfeifer D, Engelhardt KR, Rezaei N, Grimbacher B, Lohrmann S, Sherkat R and Klein C. The phenotype of human STK4 deficiency. *Blood*. 2012;119:3450-7.
23. Dang TS, Willet JD, Griffin HR, Morgan NV, O'Boyle G, Arkwright PD, Hughes SM, Abinun M, Tee LJ, Barge D, Engelhardt KR, Jackson M, Cant AJ, Maher ER, Koref MS, Reynard LN, Ali S and Hambleton S. Defective Leukocyte Adhesion and Chemotaxis Contributes to Combined Immunodeficiency in Humans with Autosomal Recessive MST1 Deficiency. *J Clin Immunol*. 2016;36:117-22.
24. Liu MM, Yan M, Lv HZ, Wang BQ, Lv X, Zhang H, Xiang S, Du J, Liu T, Tian YK, Zhang X, Zhou FF, Cheng T, Zhu Y, Jiang HF, Cao YH and Ai D. Macrophage K63-Linked Ubiquitination of YAP Promotes Its Nuclear Localization and Exacerbates Atherosclerosis. *Cell Reports*. 2020;32.
25. Wang L, Yu P, Zhou B, Song J, Li Z, Zhang M, Guo G, Wang Y, Chen X, Han L and Hu S. Single-cell reconstruction of the adult human heart during heart failure and recovery reveals the cellular landscape underlying cardiac function. *Nat Cell Biol*. 2020;22:108-119.

26. Li W, Xiao J, Zhou X, Xu M, Hu C, Xu X, Lu Y, Liu C, Xue S, Nie L, Zhang H, Li Z, Zhang Y, Ji F, Hui L, Tao W, Wei B and Wang H. STK4 regulates TLR pathways and protects against chronic inflammation-related hepatocellular carcinoma. *J Clin Invest*. 2015;125:4239-54.
27. Maj T, Wang W, Crespo J, Zhang H, Wei S, Zhao L, Vatan L, Shao I, Szeliga W, Lyssiotis C, Liu JR, Kryczek I and Zou W. Oxidative stress controls regulatory T cell apoptosis and suppressor activity and PD-L1-blockade resistance in tumor. *Nat Immunol*. 2017;18:1332-1341.
28. Serhan CN. Pro-resolving lipid mediators are leads for resolution physiology. *Nature*. 2014;510:92-101.
29. Sun AR, Wu X, Liu B, Chen Y, Armitage CW, Kollipara A, Crawford R, Beagley KW, Mao X, Xiao Y and Prasadam I. Pro-resolving lipid mediator ameliorates obesity induced osteoarthritis by regulating synovial macrophage polarisation. *Sci Rep*. 2019;9:426.
30. Dincbas-Renqvist V, Pepin G, Rakonjac M, Plante I, Ouellet DL, Hermansson A, Goulet I, Doucet J, Samuelsson B, Radmark O and Provost P. Human Dicer C-terminus functions as a 5-lipoxygenase binding domain. *Biochim Biophys Acta*. 2009;1789:99-108.
31. Bateman A and Sandford R. The PLAT domain: a new piece in the PKD1 puzzle. *Curr Biol*. 1999;9:R588-90.
32. Flamand N, Luo M, Peters-Golden M and Brock TG. Phosphorylation of serine 271 on 5-lipoxygenase and its role in nuclear export. *J Biol Chem*. 2009;284:306-13.
33. Luo M, Jones SM, Flamand N, Aronoff DM, Peters-Golden M and Brock TG. Phosphorylation by protein kinase a inhibits nuclear import of 5-lipoxygenase. *J Biol Chem*. 2005;280:40609-16.
34. Gerstmeier J, Newcomer ME, Dennhardt S, Romp E, Fischer J, Werz O and Garscha U. 5-Lipoxygenase-activating protein rescues activity of 5-lipoxygenase mutations that delay nuclear membrane association and disrupt product formation. *FASEB J*. 2016;30:1892-900.
35. Radmark O, Werz O, Steinhilber D and Samuelsson B. 5-Lipoxygenase, a key enzyme for leukotriene biosynthesis in health and disease. *Biochim Biophys Acta*. 2015;1851:331-9.
36. Garscha U, Romp E, Pace S, Rossi A, Temml V, Schuster D, Konig S, Gerstmeier J, Liening S, Werner M, Atze H, Wittmann S, Weinigel C, Rummler S, Scriba GK, Sautebin L and Werz O. Pharmacological profile and efficiency in vivo of diflapolin, the first dual inhibitor of 5-lipoxygenase-activating protein and soluble epoxide hydrolase. *Sci Rep*. 2017;7:9398.
37. Werz O, Gerstmeier J, Libreros S, De la Rosa X, Werner M, Norris PC, Chiang N and Serhan CN. Human macrophages differentially produce specific resolvin or leukotriene signals that depend on bacterial pathogenicity. *Nat Commun*. 2018;9:59.
38. Wan E, Yeap XY, Dehn S, Terry R, Novak M, Zhang S, Iwata S, Han X, Homma S, Drosatos K, Lomasney J, Engman DM, Miller SD, Vaughan DE, Morrow JP, Kishore R and Thorp EB. Enhanced efferocytosis of apoptotic cardiomyocytes through myeloid-epithelial-reproductive tyrosine kinase links acute inflammation resolution to cardiac repair after infarction. *Circ Res*. 2013;113:1004-12.
39. Tang J, Shen Y, Chen G, Wan Q, Wang K, Zhang J, Qin J, Liu G, Zuo S, Tao B, Yu Y, Wang J, Lazarus M and Yu Y. Activation of E-prostanoid 3 receptor in macrophages facilitates cardiac healing after myocardial infarction. *Nature communications*. 2017;8:14656.
40. Fan F, He Z, Kong LL, Chen Q, Yuan Q, Zhang S, Ye J, Liu H, Sun X, Geng J, Yuan L, Hong L, Xiao C, Zhang W, Li Y, Wang P, Huang L, Wu X, Ji Z, Wu Q, Xia NS, Gray NS, Chen L, Yun CH,

Deng X and Zhou D. Pharmacological targeting of kinases MST1 and MST2 augments tissue repair and regeneration. *Sci Transl Med*. 2016;8:352ra108.
41. Triastuti E, Nugroho AB, Zi M, Prehar S, Kohar YS, Bui TA, Stafford N, Cartwright EJ, Abraham S and Oceandy D. Pharmacological inhibition of Hippo pathway, with the novel kinase inhibitor XMU-MP-1, protects the heart against adverse effects during pressure overload. *Br J Pharmacol*. 2019;176:3956-3971.
42. Shi H, Liu C, Tan H, Li Y, Nguyen TM, Dhungana Y, Guy C, Vogel P, Neale G, Rankin S, Feng Y, Peng J, Tao W and Chi H. Hippo Kinases Mst1 and Mst2 Sense and Amplify IL-2R-STAT5 Signaling in Regulatory T Cells to Establish Stable Regulatory Activity. *Immunity*. 2018;49:899-914 e6.
43. Nehme NT, Schmid JP, Debeurme F, Andre-Schmutz I, Lim A, Nitschke P, Rieux-Laucat F, Lutz P, Picard C, Mahlaoui N, Fischer A and de Saint Basile G. MST1 mutations in autosomal recessive primary immunodeficiency characterized by defective naive T-cell survival. *Blood*. 2012;119:3458-68.
44. Wang P, Geng J, Gao J, Zhao H, Li J, Shi Y, Yang B, Xiao C, Linghu Y, Sun X, Chen X, Hong L, Qin F, Li X, Yu JS, You H, Yuan Z, Zhou D, Johnson RL and Chen L. Macrophage achieves self-protection against oxidative stress-induced ageing through the Mst-Nrf2 axis. *Nat Commun*. 2019;10:755.
45. Dixon RA, Diehl RE, Opas E, Rands E, Vickers PJ, Evans JF, Gillard JW and Miller DK. Requirement of a 5-lipoxygenase-activating protein for leukotriene synthesis. *Nature*. 1990;343:282-4.
46. Woods JW, Evans JF, Ethier D, Scott S, Vickers PJ, Hearn L, Heibein JA, Charleson S and Singer, II. 5-lipoxygenase and 5-lipoxygenase-activating protein are localized in the nuclear envelope of activated human leukocytes. *J Exp Med*. 1993;178:1935-46.
47. Brock TG, McNish RW, Bailie MB and Peters-Golden M. Rapid import of cytosolic 5-lipoxygenase into the nucleus of neutrophils after in vivo recruitment and in vitro adherence. *J Biol Chem*. 1997;272:8276-80.
48. Brock TG, Anderson JA, Fries FP, Peters-Golden M and Sporn PH. Decreased leukotriene C4 synthesis accompanies adherence-dependent nuclear import of 5-lipoxygenase in human blood eosinophils. *J Immunol*. 1999;162:1669-76.
49. Luo M, Jones SM, Peters-Golden M and Brock TG. Nuclear localization of 5-lipoxygenase as a determinant of leukotriene B4 synthetic capacity. *Proc Natl Acad Sci U S A*. 2003;100:12165-70.
50. Mandal AK, Jones PB, Bair AM, Christmas P, Miller D, Yamin TT, Wisniewski D, Menke J, Evans JF, Hyman BT, Bacskai B, Chen M, Lee DM, Nikolic B and Soberman RJ. The nuclear membrane organization of leukotriene synthesis. *Proc Natl Acad Sci U S A*. 2008;105:20434-9.
51. Cheung WL, Ajiro K, Samejima K, Kloc M, Cheung P, Mizzen CA, Beeser A, Etkin LD, Chernoff J, Earnshaw WC and Allis CD. Apoptotic phosphorylation of histone H2B is mediated by mammalian sterile twenty kinase. *Cell*. 2003;113:507-17.
52. Kain V, Ingle KA, Kabarowski J, Barnes S, Limdi NA, Prabhu SD and Halade GV. Genetic deletion of 12/15 lipoxygenase promotes effective resolution of inflammation following myocardial infarction. *J Mol Cell Cardiol*. 2018;118:70-80.
53. Lammermann T, Afonso PV, Angermann BR, Wang JM, Kastenmuller W, Parent CA and Germain RN. Neutrophil swarms require LTB4 and integrins at sites of cell death in vivo. *Nature*. 2013;498:371-5.

54. Kurz AR, Pruenster M, Rohwedder I, Ramadass M, Schafer K, Harrison U, Gouveia G, Nussbaum C, Immler R, Wiessner JR, Margraf A, Lim DS, Walzog B, Dietzel S, Moser M, Klein C, Vestweber D, Haas R, Catz SD and Sperandio M. MST1-dependent vesicle trafficking regulates neutrophil transmigration through the vascular basement membrane. *J Clin Invest*. 2016;126:4125-4139.
55. Fredman G, Ozcan L, Spolitu S, Hellmann J, Spite M, Backs J and Tabas I. Resolvin D1 limits 5-lipoxygenase nuclear localization and leukotriene B4 synthesis by inhibiting a calcium-activated kinase pathway. *Proc Natl Acad Sci U S A*. 2014;111:14530-5.
56. Geng J, Sun X, Wang P, Zhang S, Wang X, Wu H, Hong L, Xie C, Li X, Zhao H, Liu Q, Jiang M, Chen Q, Zhang J, Li Y, Song S, Wang HR, Zhou R, Johnson RL, Chien KY, Lin SC, Han J, Avruch J, Chen L and Zhou D. Kinases Mst1 and Mst2 positively regulate phagocytic induction of reactive oxygen species and bactericidal activity. *Nat Immunol*. 2015;16:1142-52.
57. Reichert K, Colantuono B, McCormack I, Rodrigues F, Pavlov V and Abid MR. Murine Left Anterior Descending (LAD) Coronary Artery Ligation: An Improved and Simplified Model for Myocardial Infarction. *J Vis Exp*. 2017.
58. Thygesen K, Alpert JS, Jaffe AS, Chaitman BR, Bax JJ, Morrow DA, White HD and Executive Group on behalf of the Joint European Society of Cardiology /American College of Cardiology /American Heart Association /World Heart Federation Task Force for the Universal Definition of Myocardial I. Fourth Universal Definition of Myocardial Infarction (2018). *Circulation*. 2018;138:e618-e651.
59. Zhou X, Li W, Wang S, Zhang P, Wang Q, Xiao J, Zhang C, Zheng X, Xu X, Xue S, Hui L, Ji H, Wei B and Wang H. YAP Aggravates Inflammatory Bowel Disease by Regulating M1/M2 Macrophage Polarization and Gut Microbial Homeostasis. *Cell Rep*. 2019;27:1176-1189.e5.
60. Yao F, Yu P, Li Y, Yuan X, Li Z, Zhang T, Liu F, Wang Y, Wang Y, Li D, Ma B, Shu C, Kong W, Zhou B and Wang L. Histone Variant H2A.Z Is Required for the Maintenance of Smooth Muscle Cell Identity as Revealed by Single-Cell Transcriptomics. *Circulation*. 2018;138:2274-2288.
61. Goldstein LD, Chen YJ, Dunne J, Mir A, Hubschle H, Guillory J, Yuan W, Zhang J, Stinson J, Jaiswal B, Pahuja KB, Mann I, Schaal T, Chan L, Anandakrishnan S, Lin CW, Espinoza P, Husain S, Shapiro H, Swaminathan K, Wei S, Srinivasan M, Seshagiri S and Modrusan Z. Massively parallel nanowell-based single-cell gene expression profiling. *BMC Genomics*. 2017;18:519.
62. Langmead B and Salzberg SL. Fast gapped-read alignment with Bowtie 2. *Nat Methods*. 2012;9:357-9.
63. Dobin A, Davis CA, Schlesinger F, Drenkow J, Zaleski C, Jha S, Batut P, Chaisson M and Gingeras TR. STAR: ultrafast universal RNA-seq aligner. *Bioinformatics*. 2013;29:15-21.
64. Liao Y, Smyth GK and Shi W. featureCounts: an efficient general purpose program for assigning sequence reads to genomic features. *Bioinformatics*. 2014;30:923-30.
65. Wolock SL, Lopez R and Klein AM. Scrublet: Computational Identification of Cell Doublets in Single-Cell Transcriptomic Data. *Cell Syst*. 2019;8:281-291.e9.
66. Stuart T, Butler A, Hoffman P, Hafemeister C, Papalexi E, Mauck WM, 3rd, Hao Y, Stoeckius M, Smibert P and Satija R. Comprehensive Integration of Single-Cell Data. *Cell*. 2019;177:1888-1902.e21.

67. Zhang X, Yang N, Ai D and Zhu Y. Systematic metabolomic analysis of eicosanoids after omega-3 polyunsaturated fatty acid supplementation by a highly specific liquid chromatography-tandem mass spectrometry-based method. *J Proteome Res*. 2015;14:1843-53.
68. Li W, Xiao J, Zhou X, Xu M, Hu C, Xu X, Lu Y, Liu C, Xue S, Nie L, Zhang H, Li Z, Zhang Y, Ji F, Hui L, Tao W, Wei B and Wang H. STK4 regulates TLR pathways and protects against chronic inflammation-related hepatocellular carcinoma. *J Clin Invest*. 2015;125:4239-54.
69. Maj T, Wang W, Crespo J, Zhang H, Wang W, Wei S, Zhao L, Vatan L, Shao I, Szeliga W, Lyssiotis C, Liu JR, Kryczek I and Zou W. Oxidative stress controls regulatory T cell apoptosis and suppressor activity and PD-L1-blockade resistance in tumor. *Nat Immunol*. 2017;18:1332-1341.

FIGURE LEGENDS

Fig. 1. Macrophage MST1/2 deficiency aggravates injury from myocardial infarction (MI) in mice.
(**A**) Expression of Mst1 in cardiac macrophages from wild-type mice at indicated times after MI was measured by flow cytometry. *P*-values correspond to Kruskal-Wallis with Dunn's multiple comparisons test (n = 5). (**B–D**) MI surgery was performed in *Mst1/2*$^{flox/flox}$ mice and *LysMCre-Mst1/2*$^{flox/flox}$ knockout mice, which were then assessed on Day 0, 3, and 7 post-MI. (**B**) Representative M-mode echocardiographic images. (**C**) Quantification of left ventricular (LV) ejection fraction (EF), fraction shortening (FS), LV end-diastolic volume (LVEDV) and LV end-systolic volume (LVESV) by echocardiographic analysis (n = 6). *P*-values correspond to two-way ANOVA with Tukey's multiple comparisons test. (**D**) Numbers of macrophages in mouse hearts, *P*-values correspond to Kruskal-Wallis with Dunn's multiple comparisons test (n = 5). (**E–G**) Single cells were isolated from the hearts of *Mst1/2*$^{flox/flox}$ and *LysMCre-Mst1/2*$^{flox/flox}$ mice on Day 3 post-MI and subjected to single-cell RNA sequencing. (**E**) Uniform Manifold Approximation and Projection (UMAP) visualize the clustering of 867 immune cells identified from *Mst1/2*$^{flox/flox}$ and *LysMCre-Mst1/2*$^{flox/flox}$ mice, labelled by cell type (left) and genetic background (right). Cell types were determined by the expression of known markers. MP, macrophage; B, B cell; GR, granulocyte; T, T cell. (**F**) Violin plots show specifically expressed genes (SEGs) expression in MP clusters. (**G**) MP subtype proportions in all macrophages from hearts of *Mst1/2*$^{flox/flox}$ and *LysMCre-Mst1/2*$^{flox/flox}$ mice. (**H**) mRNA levels of SEGs in heart tissues, examined by quantitative PCR in *Mst1/2*$^{flox/flox}$ and *LysMCre-Mst1/2*$^{flox/flox}$ mice on Day 3 post-MI. The data are normalized to *β-actin* and expressed as the fold change over the values of *Mst1/2*$^{flox/flox}$ mice, *P*-values correspond to Mann-Whitney U test (n = 5).

Fig. 2. MST1 deficiency induces LTB4 production in macrophages.
(**A**) Wild-type (WT) murine peritoneal macrophages were treated for 6 h with conditioned media (CM) from the culture of *Mst1*$^{+/+}$ or *Mst1*$^{-/-}$ macrophages. CM was untreated (ctrl), trypsinized (trypsin) to remove proteins, or treated with dextran-coated charcoal (DCC) to remove small molecules. mRNA levels of *Ccl2* and *Ccl4* were measured by quantitative PCR. *P*-values correspond to unpaired two-tailed *t* test. (n = 6). (**B–F**) Liquid chromatography–tandem mass spectrometry (LC-MS/MS) detected polyunsaturated-fatty-acid-derived metabolites in CM from *Mst1*$^{+/+}$ and *Mst1*$^{-/-}$ macrophages. (**B**) An orthogonal PLS-DA model was built based on metabolite measurements. (**C**) Heatmap of CM levels of lipid mediators from *Mst1*$^{+/+}$ and *Mst1*$^{-/-}$ macrophages (n = 5). (**D**) Features (variables) of top 10 most significant metabolites based on VIP scores from PLS-DA. The x-axis shows correlation scores and the y-axis shows the metabolites. (**E**) Volcano plot showing fold change of metabolites level between *Mst1*$^{+/+}$ and *Mst1*$^{-/-}$ macrophages (n = 5). Metabolites significantly upregulated in *Mst1*$^{-/-}$ macrophages are labelled. (**F**) Quantification of selected lipid mediators, *P*-values correspond to Mann-Whitney U test (n = 5). (**G**) Quantification of LTB4 by ELISA in heart tissue from *LysMCre-Mst1/2*$^{flox/flox}$ and *Mst1/2*$^{flox/flox}$ mice on Day 3 post-MI. *P*-values correspond to Mann-Whitney U test (n= 5). (**H**) Quantification of plasma levels of LTB4 by LC-MS in STEMI patients (n = 118) and control individuals (n = 119). *P*-values correspond to unpaired two-tailed *t* test.

Fig. 3. MST1 phosphorylates 5-LOX at T218.
(**A**) Immunoblotting analysis of 5-LOX and MST1 in peritoneal macrophages from *Mst1*$^{+/+}$ and *Mst1*$^{-/-}$ mice, *P*-values correspond to unpaired two-tailed *t* test (n = 6). (**B**) Quantitative PCR analysis of *Alox5* mRNA levels in peritoneal macrophages from *Mst1*$^{+/+}$ and *Mst1*$^{-/-}$ mice, *P*-values correspond to Mann-Whitney U test (n = 5). (**C–G**) Co-immunoprecipitation of 5-LOX with MST1. (**C**) HEK293T cells

were transfected with plasmids expressing Myc-MST1 and/or Flag-5-LOX for 48 h. Immunoprecipitation was performed with anti-Myc antibody (IP: Myc) or IgG (IP: IgG), followed by immunoblotting with anti-Flag and anti-Myc antibodies (n = 5). (**D**) HEK293T cells were transfected with plasmids expressing Myc-MST1 and either Flag-5-LOX or Flag-5-LOX$^{\Delta PLAT}$ (a PLAT-domain deletion variant), followed by immunoprecipitation with anti-Flag (IP: Flag) and immunoblotting with anti-Flag and anti-Myc antibodies (n = 5). (**E**) Amino acid sequence alignment of 5-LOX orthologs (above). Mass spectrometry (MS) of 5-LOX phosphorylated by MST1 indicated phosphorylation at S216, T218 or T418 (below). (**F**) HEK293T cells were transfected with plasmids expressing Myc-MST1 and Flag-tagged 5-LOX or its variants (S216A, T218A, and T428A) for 48 h. Immunoprecipitation was performed with anti-Flag (IP: Flag), followed by immunoblotting with anti-Flag, anti-Myc, anti-p-S/T/Y, and anti-p-5LOX^{T218} antibodies (n = 5). (**G**) HEK293T cells were transfected with plasmids encoding Flag-5-LOX, Myc-MST1^{K59R}, Myc-MST1 (at various doses), or with an empty vector for 48 h. Immunoprecipitation was performed with anti-Flag (IP: Flag) or IgG (IP: IgG), followed by immunoblotting with anti-Flag, anti-Myc, or anti-p-5LOX^{T218} antibodies. (**H**) Quantification of total phosphorylated 5-LOX^{T218}. P-values correspond to Kruskal-Wallis with Dunn's multiple comparisons test (n = 5).

Fig. 4. 5-LOX^{T218A} promotes 5-LOX/FLAP nuclear-membrane interaction.
(**A**) HEK293T cells were transfected with plasmids directing expression of the indicated proteins for 48 h. LTB4 was measured in intact cells or homogenates by LC-MS/MS. P-values correspond to one-way ANOVA with Tukey's multiple comparisons test (n = 6). (**B–C**) HEK293T cells were transfected with plasmids directing expression of the indicated proteins for 48 h, then treated with or without calcium ionophore A23187 (2.5 μM) for 30 min at 37°C. (**B**) Representative immunofluorescence staining of 5-LOX (red), FLAP (green), and DAPI (blue). (**C**) In situ proximity ligation assay (PLA) was performed with proximity probes against 5-LOX and FLAP. Nuclei were stained with DAPI (blue), and in situ PLA signals (red) visualized 5-LOX–FLAP interactions. (**D**) Monocytes were isolated from *Mst1/2$^{flox/flox}$* and *LysMCre-Mst1/2$^{flox/flox}$* mice. PLA was performed to detect 5-LOX–FLAP interactions. Results shown in panel B, C, and D for one single cell are representative of ~100 individual cells analyzed in three independent experiments. (**E**) HEK293T cells were transfected with plasmids directing the expression of the indicated proteins for 48 h. LTB4 was measured in intact cells or homogenates by LC-MS/MS. P-values correspond to one-way ANOVA with Tukey's multiple comparisons test (n = 6).

Fig. 5. The LTB4–BLT1 axis contributes to MST1-deficiency-induced inflammation in macrophages.
(**A–C**) Wild-type (WT) peritoneal macrophages were pretreated with vehicle only or CP105696 at 10 μM for 1 h, then given no further treatment or stimulated with LTB4 (100 nM) for 6 h (**A**) or 1 h (**B**). (**A**) mRNA levels of markers specific to three macrophage subtypes were assessed by quantitative PCR, P-values correspond to two-way ANOVA with Tukey's multiple comparisons test (n = 6). (**B–C**) Immunoblotting analysis and ratios of proteins to phosphoproteins, P-values correspond to Kruskal-Wallis with Dunn's multiple comparisons test (n = 5). (**D–F**) Peritoneal macrophages were pretreated with 10 μM CP105696 (or vehicle) for 1 h, and then treated with conditioned media (CM) from *Mst1$^{+/+}$* or *Mst1$^{-/-}$* peritoneal macrophages for 6 h (**D**) or 1 h (**E**). (**D**) Macrophage subtype marker-gene expression was measured by PCR, P-values correspond to two-way ANOVA with Tukey's multiple comparisons test (n = 6). (**E–F**) Immunoblotting analysis and ratios of proteins to phosphoproteins, P-values correspond to Kruskal-Wallis with Dunn's multiple comparisons test (n = 5).

Fig. 6. BLT1 antagonist ameliorates MST1/2-conditional-knockout-induced cardiac dysfunction after myocardial infarction (MI).
Mst1/2$^{flox/flox}$ and *LysMCre-Mst1/2$^{flox/flox}$* mice were administrated with vehicle or CP105696 (100 mg/kg daily by oral gavage) for 1 week then subjected to MI surgery. (**A**) Representative M-mode echocardiograms obtained on Day 0, 1 and 28 after MI from mice in indicated groups. (**B**) Echocardiographic measurements of ejection fraction (EF), fractional shortening (FS), left ventricular

end-diastolic volume (LVEDV), and left ventricular end-systolic volume (LVESV) in indicated groups on Day 0, 1, 3, 7, 28 post-MI (n = 6), P-values correspond to two-way ANOVA with Tukey's multiple comparisons test, * *LysMCre-Mst1/2*$^{flox/flox}$ + Vehicle vs *Mst1/2* $^{flox/flox}$ + Vehicle; # *LysMCre-Mst1/2*$^{flox/flox}$ + CP vs *LysMCre-Mst1/2*$^{flox/flox}$ + Vehicle. (**C**) Summarized data of heart weight/body weight (HW/BW), lung weight/body weight (LW/BW) of MI-operated mice 28 days after surgery (n = 6). (**D**) Post-MI survival analysis, n = 23 per group. (**E**) Masson's trichrome staining of sequential heart cross sections from each block were cut at 200 μm intervals in indicated groups on Day 28 after MI (n = 6). (**F**) Summarized data of infarct size measured from sequential sections in E (n = 6). (**G**) Immunofluorescence staining of CD31 (red) and DAPI (blue) in cross-sections of mouse hearts in indicated groups on Day 28 after MI. (**H**) Quantitative analysis of CD31 positive cells in border areas of hearts in G (n = 6) (**I**) mRNA levels in heart tissues were examined by quantitative PCR on Day 7 post MI. Data were normalized to *β-actin* and expressed as fold-change over the values for *Mst1/2*$^{flox/flox}$ mice treated with vehicle (n = 6). (C, F, H, I) P-values correspond to two-way ANOVA with Tukey's multiple comparisons test. The survival rate was analyzed by Kaplan-Meier method and compared by log-rank test (D).

Fig. 7. Combination therapy with CP105696 and XMU-MP-1 alleviates injury from myocardial infarction (MI).

Wild-type (WT) mice were administrated with vehicle, CP105696 (100 mg/kg daily by oral gavage), XMU-MP-1 (1mg/kg every other day by intraperitoneal injection) or combined CP105696 and XMU-MP-1 for 1 week then subjected to MI surgery. (**A**) Representative M-mode echocardiograms obtained on Day 0, 1 and 28 after MI from mice in indicated groups. (**B**) Echocardiographic measurements of ejection fraction (EF), fractional shortening (FS), left ventricular end-diastolic volume (LVEDV), and left ventricular end-systolic volume (LVESV) in indicated groups on Day 0, 1, 3, 7, 28 post-MI (n = 6), P-values correspond to two-way ANOVA with Tukey's multiple comparisons test, * XMU vs Vehicle; # XMU + CP vs XMU; § XMU + CP vs CP. (**C**) Summarized data of heart weight/body weight (HW/BW), lung weight/body weight (LW/BW) for MI-operated mice 28 days after surgery (n = 6). (**D**) Post-MI survival analysis, n = 25 per group. (**E**) Masson's trichrome staining of sequential heart cross-sections from each block was cut at 200 μm intervals in indicated groups on Day 28 after MI (n = 6). (**F**) Summarized data of infarct size measured from sequential sections in E (n = 6). (**G**) Immunofluorescence staining of CD31 (red) and DAPI (blue) in cross-sections of mouse hearts in indicated groups on Day 28 after MI. (H) Quantitative analysis of CD31 positive cells in border areas of hearts in G (n = 6) (**I**) mRNA levels in heart tissues were examined by quantitative PCR on Day7 post MI. Data were normalized to *β-actin* and expressed as fold-change over the values for WT mice treated with vehicle (n = 6). (C, H, F, I) P-values correspond to one-way ANOVA with Tukey's multiple comparisons test. The survival rate was analyzed by Kaplan-Meier method and compared by log-rank test (D).

NOVELTY AND SIGNIFICANCE

What Is Known?

- Acute myocardial infarction (MI) is one of the most frequent causes of myocardial injury. Timely suppression of inflammation is important to post-infarction cardiac repair.

- Mammalian STE20-like protein kinase 1/2 (MST1/2), which is the major component of the mammalian Hippo signaling pathway, acts as a regulator of macrophage-associated immune responses to bacterial infections.

What New Information Does This Article Contribute?

- Macrophage-specific deficiency of MST1/2 aggravated MI injury in mice via induction of LTB4 production and promotion of macrophage subtype switching to a proinflammatory profile.

- MST1-mediated 5-LOX phosphorylation at T218 disrupted the interaction between 5-LOX and FLAP and thus inhibited LTB4 production.

- Inhibition of BLT1 with CP105696 improved the cardiac dysfunction in mice with genetic or pharmacological inhibition of Mst1/2 after MI.

Inflammation and inflammatory cell infiltration are the hallmarks of MI, which is the most common cause of cardiac injury. Overactive, prolonged, or spatially expanded inflammatory reactions lead to serious damage and dysfunction. In the present study, we investigate the role of macrophage MST1/2 in MI injury and found that the MST1–5-LOX–LTB4–BLT1 axis is a key regulator of cardiac repair post-MI. We identified 5-LOX as a novel substrate of MST1 kinase and assessed a therapeutic combination of the MST1/2 inhibitor and tissue-repair drug XMU-MP-1 with the BLT1 antagonist CP105696, which can overcome negative inflammatory consequences of treatment with XMU-MP-1 alone and thus ameliorate MI injury and prevent heart failure.